[23] E. G. Pan, A. A. Ravaev, *Adv. Eng. Mater.* **2004**, *6*, 61.
[24] G. Neite, K. Kubota, K. Higashi, F. Hehmann, in *Mater. Sci. and Technol. Vol. 8*, Wiley-VCH, Germany, **2005**, 115–212.

DOI: 10.1002/adem.200600008

Processing, Microstructure and Mechanical Properties of in Situ Al-based Metal Matrix Composite Reinforced with 22 wt%WAl_{12} Particles**

By *Shuguang Cai, Xianfeng Ma,* Huaguo Tang, Wei Zhao, Changjun Zhu, Junmin Yan, Zhuhui Qiao, Bo Zhao*

In the past decade, Al-based metal matrix composite (MMC) reinforced with particles has been received much attention due to its high elastic modulus, high strength and light weight that is of value to automobile and aerospace industries, etc.[1] Very recently, Yu et al[2] reported the structure and characterization of an in situ Al-based MMC reinforced with Al_2O_3 and TiC produced by hot isostatic pressing (HIP) technique, which indicated that the mechanical performance of Al-10 wt%TiO_2-1.5 wt%C is higher than that of Al-10 wt%TiO_2 due to formation of TiC and elimination of large intermetallic Al_3Ti plates. By using a mechanical alloying technique, Jia et al[3] synthesized an Al_3Ti particle and Nb flake reinforced Al matrix composite and found that the MA Al-12Ti-Nb has much more excellent mechanical properties and thermal stability than the MA Al-12Ti. Al-TiB_2 metal matrix composites prepared by exothermic reactions at 850 °C using K_2TiF_6 and KBF_4 salts and using stir cast route at above 1000 °C, respectively, have also been documented by Lu's group.[4,5]

Compared with these typical ceramic particulates, in situ intermetallic WAl_{12}, fabricated by MA and vacuum hot pressing (HP) techniques, is a new reinforcement with clean grain boundary. However, synthesis of composites with in situ WAl_{12} reinforcement has never been reported.

Mechanical alloying is a solid-state powder processing technique which was effectively employed to prepare a variety of alloy powders or blend green samples,[6–9] The hot-pressing technique is a highly evolved method of preparing full dense, good matrix-to-reinforcement compatible and microstructural homogeneous materials. Therefore, MMCs can be well synthesized by using the in situ technique.[3]

In this paper, we focus on fabricating in situ WAl_{12} reinforced Al-based MMC via MA and HP using $W_{14}Al_{86}$ alloy, which is of high microhardness, good oxidation resistance and low density, etc.[10] The mechanical properties and the microstructures of the MMC were also determined.

Results and discussion. Synthesis of $W_{14}Al_{86}$ alloy: The aluminum and tungsten powders were mixed to give a desired composition of $W_{14}Al_{86}$ and mechanically milled for 10, 30, 50 and 70 h respectively in a stainless steel vial filled with argon. Figure 1 shows a series of XRD patterns indicating the phase evolution as a function of milling time in the mixture. The as-received elemental blend showed the presence of both elemental aluminum and tungsten phases clearly. As milling time increased, intensity of Al peaks decreased continuously. After 70 h milling, Al peaks disappeared, whereas W peaks were still visible. It implied that Al completely dissolved in the remaining bcc W-based phase, indicating that $W_{14}Al_{86}$ alloy was prepared by mechanical alloying process.

Formation of in situ WAl_{12} reinforcement: Figure 2 shows the typical XRD patterns of the HPed Al-15 wt%$W_{14}Al_{86}$ samples under various sintering conditions. After sintering at 600 ⊖ for 30 min (Fig. 2(a)), the diffraction peaks of $W_{14}Al_{86}$ alloy still existed and no WAl_{12} diffraction peaks appeared. How-

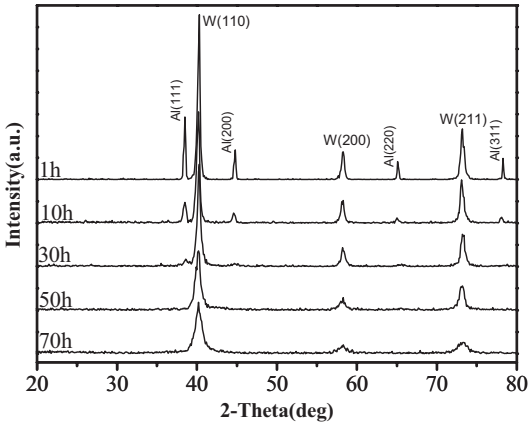

Fig. 1. XRD patterns of the MA-ed $W_{14}Al_{86}$ powders after various milling time.

[*] *Dr. S. Cai, Prof. X. F. Ma, Dr. H. Tang, Prof. W. Zhao, Dr. C. Zhu, Dr. J. M. Yan, Dr. Z. Qiao, Dr. B. Zhao*
Changchun Institute of Applied Chemistry
Chinese Academy of Sciences
Graduate School of Chinese Academy of Sciences
Changchun 130022, PR China
E-mail: xfma@ ciac.jl.cn (X. F. Ma)

[**] *The authors thank the financial support provided by Jilin Province, China through a project of Science and Technology Development Program, 20030508. In addition, the funding of this project (50371080) from the National Natural Science Foundation of China also is gratefully acknowledgement.*

ADVANCED ENGINEERING MATERIALS

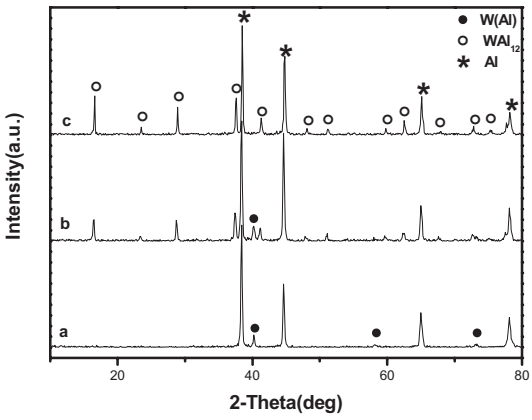

Fig. 2. XRD patterns of Al-15 wt% $W_{14}Al_{86}$ composite obtained under various conditions.(a)600 °C, 30 min (b) 650 °C, 5 min (c) 650 °C, 30 min.

ever, after sintering at 650 °C for 5 min (Fig. 2(b)), the diffraction peaks of WAl_{12} began to appear, at the same time, intensities of $W_{14}Al_{86}$ alloy diffraction peaks decreased but not disappeared completely. When the sintering time lasted 30 min at 650 °C (Fig. 2(c)), the $W_{14}Al_{86}$ peaks completely disappeared with further enhancement of WAl_{12} peaks. Therefore, it was reasonable to expect $W_{14}Al_{86}$ alloy reacting with Al atoms to form the WAl_{12} intermetallic phase at 650–690 °C according to Al-W phase diagram.[11] Thus, it could be preliminarily demonstrated that the HPed Al-15 wt%$W_{14}Al_{86}$ specimen was an in situ Al-based MMC reinforced with 22 wt% intermetallic WAl_{12}.

Densities and microhardnesses of HP-ed Al-15wt%$W_{14}Al_{86}$ specimens: The relative density and microhardness measurements of the HPed Al-15 wt%$W_{14}Al_{86}$ specimens sintered under various conditions are given in Table 1. As shown in Figure 1, with the dissolving of Al in W, the position of XRD peak of W(Al) phase hardly changed, and according to the Rietveld analysis results of XRD pattern, the lattice parameter of W(Al) phase did not change significantly and kept at 3.1648 Å. The calculated theoretical density of BCC $W_{14}Al_{86}$ alloy was 5.13 g/cm^3. Accordingly, the densities of these specimens could be attained. The relative density of C5 reached 99.97 % and was the highest value among these specimens except that the density of C6 was a degree greater than the full density due to sintering temperature beyond melting point of aluminum leading to loss of the molten aluminum from the matrix. As shown in Table 1, it also implied that the microhardness values (at 100 g load) seemed to be correlated with densities of these specimens and the amount of formed reinforcement in them. Therefore, it indicated that it was adequate for sintering Al-15 wt%$W_{14}Al_{86}$ specimen at 650 °C for 30 min.

Table 1. Mechanical properties, density and microhardness measurements of Al-15 wt% $W_{14}Al_{86}$ sintered under various conditions.

Specimen specification	Sintering condition (25MPa)	Relative density(%)	Microhardness (GPa)	UTS (MPa)	Young's Modulus (GPa)
C1	450 °C, 30min	94.81	1.02	202	61
C2	500 °C, 30min	96.23	1.12	251	64
C3	550 °C, 30min	97.60	1.18	285	68
C4	600 °C, 30min	98.22	1.32	372	70
C5	650 °C, 30min	99.97	1.58	487	75
C6	690 °C, 30min	100	1.71	451	78
C7	650 °C, 10min	99.02	1.42	436	72
C8	650 °C, 5min	98.58	1.30	381	70

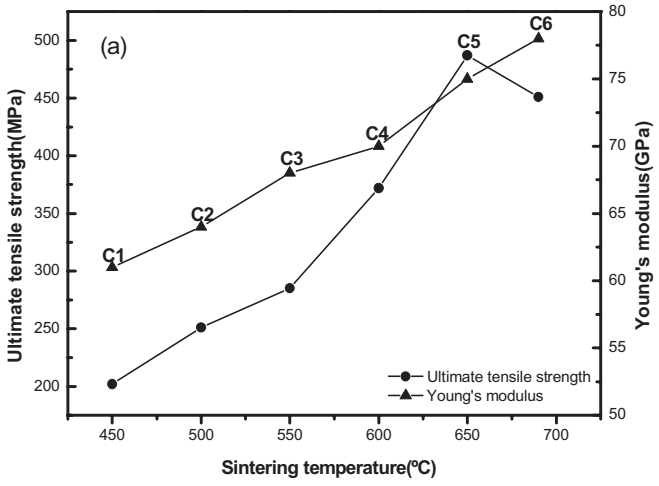

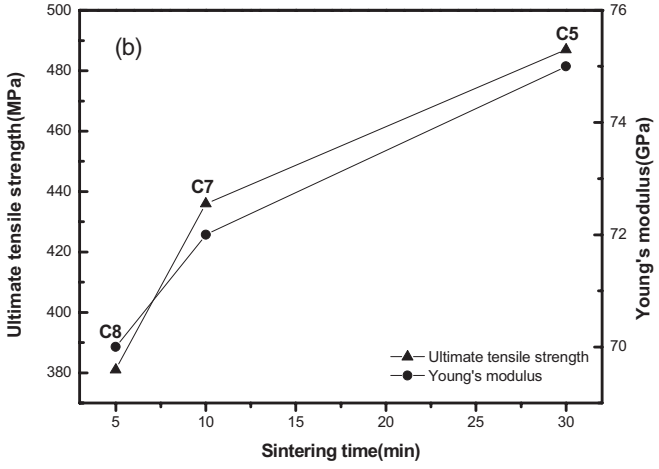

Fig. 3. The ultimate tensile strengths and moduli of HP-ed Al-15 wt%$W_{14}Al_{86}$ specimens sintered at:(a) various temperatures and 25 MPa for 30 min and (b) 650 °C and 25 MPa for various sintering duration.

Mechanical properties of HP-ed Al-15 wt%$W_{14}Al_{86}$ specimens: Figure 3(a) shows measurements of the ultimate tensile strength and Young's modulus of HP-ed Al-15 wt%$W_{14}Al_{86}$ specimens sintered at various temperatures for 30 min. As the sintering temperatures increased from 450 to 690 °C, the ultimate tensile strength increased from 202 to 487 MPa, and then dropped to 451 MPa., at the same time, the Young's modulus of these specimens increased from 61 to 78 GPa. The relations

between the ultimate tensile strength and Young's modulus of these specimens and sintering time are presented in Figure 3(b). When the sintering duration increased from 5 to 30 min, the strength and Young's modulus increased from 381 MPa and 70 GPa to 487 MPa and 75 GPa, respectively. Accordingly, it could be concluded that the strength and Young's modulus of these specimens were significantly dependent on relative densities of sintered specimens as well as the percentage of WAl_{12} formed in the Al matrix. The maximum strength value(C5) of the specimen can be explained by the good bonding between Al matrix and reinforcement particle phases due to clean interfaces without contamination among them, the forming of reinforcements in the MMC and full densification.

Microstructure of the specimen with the maximum UTS value: Figure 4(a) and (b) are the SEM micrographs showing the microstructure of the HPed Al-15 wt%$W_{14}Al_{86}$(C5) sintered at 650 °C for 30 min. As shown in Figure 4(a), in situ formed WAl_{12} intermetallic reinforcements with size < 1 μm were dispersed continuously in the Al matrix. Its fracture surface was of the cleavage type. Figure 4(b) is a higher magnification SEM micrograph of the HPed Al-15 wt%$W_{14}Al_{86}$(C5). The observation demonstrated the effectiveness of the WAl_{12} intermetallic phase reinforcement in this MMC. Table 2 shows the results of EDX analyses for reinforcement in the specimen. The result also indicated that the formed reinforcement in C5 is WAl_{12} indeed.

Table 2. The results of EDX analyses for HPed specimen.

Specimen specification	Sintering condition	Reinforcement phase		Material composition	
		W(at%)	Al(at%)	W(at%)	Al(at%)
Al-15wt%$W_{14}Al_{86}$	650 °C, 30min	7.65	92.35	1.30	98.70

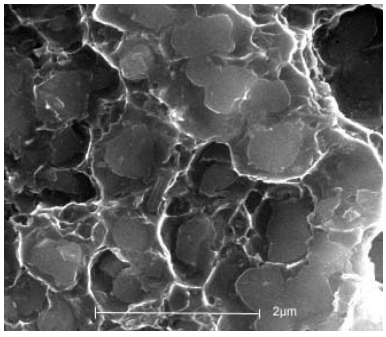

Fig. 4. (a) SEM micrograph of the HPed specimen Al-15 %$W_{14}Al_{86}$ and (b) higher magnification SEM micrograph of the HPed specimen Al-15 %$W_{14}Al_{86}$ sintered at 650 °C for 30 min under vacuum.

Contrast experiment: To validate if intermetallic WAl_{12} was formed directly from the mixture of the two metals, W and Al, in the sintering duration of 30 min, we sintered and evaluated the MA-ed mixture of Al-8 wt%W at 650 °C. The structure of the HPed Al-8 wt%W sample could be seen from the X-ray diffraction spectra shown in Figure 5. The W and Al diffraction peaks could be clearly discerned from this figure, but those of WAl_{12} were weak. It showed that a small number of WAl_{12} reinforcements forms in the short sintering duration of 30 min, because reaction velocity of $W_{14}Al_{86}$ alloy with Al was faster than that of W. However, it was necessary to form WAl_{12} reinforcements in short sintering duration in order that the grain size of the reinforcement could be controlled. The microhardness, tensile strength and Young's modulus measurements of the HPed Al-8 wt%W sample were 0.99 GPa, 130 MPa and 63 GPa, respectively. Compared with the specimen C5, the microhardness and mechanical properties of the Al-8 wt%W sample were bad due to tungsten making weak bond with aluminum and being short of good reinforcements in Al matrix. Therefore, the WAl_{12} phase could act as an effective reinforcement for promoting the Young's modulus and strength of the MMC.

Conclusions: In situ Al-22 wt%WAl_{12} composite was fabricated from Al-15 wt%$W_{14}Al_{86}$ system via mechanical alloying(MA) and vacuum hot pressing (HP). The formation of WAl_{12} particulates was confirmed by XRD and EDX studies.

The in situ preparation method used in the paper could

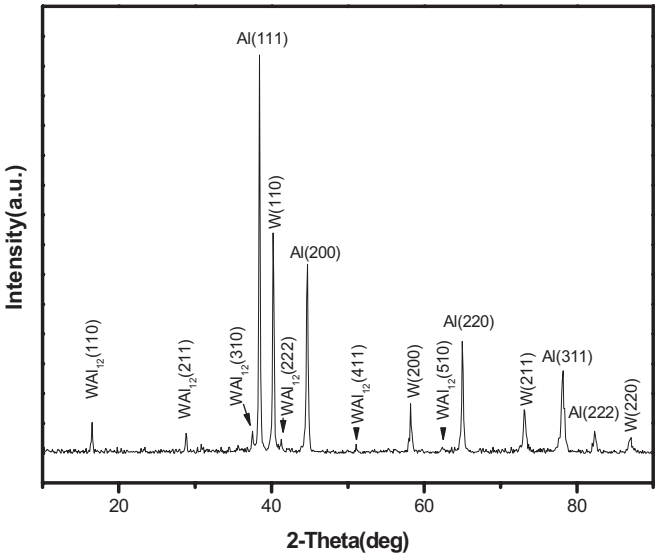

Fig. 5. The XRD pattern of Al-8 wt%W composite obtained by sintering at 650 °C for 30 min and a pressure of 25 MPa under vacuum.

produce refined WAl_{12} particulates, with a reasonably clean interface formed with aluminum matrix. The results of tensile test revealed that the incorporation of WAl_{12} to the Al matrix and full densification of the sample were beneficial to enhance the mechanical performance of in situ composite.

Compared with Al-15 wt%$W_{14}Al_{86}$ system, Al-8 wt%W system was not suitable to fabricating the in situ Al-based metal matrix composite (MMC) due to only forming a small number of reinforcements in the sintering duration of 30 min.

Experimental

Commercial grade aluminum (3.59 μm, 99.5 % purity) and tungsten (0.98 μm, 99.8 % purity) powders were used as raw materials. The $W_{14}Al_{86}$ powders were prepared in advance using a mechanical alloying technique.[10] Mechanical alloying was performed on a high-energy ball mill with a rotation speed of 580 rpm. The ball-to-powder weight ratio was 15:1. Al-15 wt% $W_{14}Al_{86}$ powders were then blended with 0.2 vol% pure alcohol, as a process control agent, in a stainless steel vial filled with argon for 1 h. In order to avoid oxidation of powders during MA treatment, all the handling were performed under argon atmosphere in a glove box. The blended powders were then cold-pressed in a steel die under a pressure of 250 MPa to form green samples with a dimension of ~ 40 mm × 20 mm × 10 mm.

The green samples were enclosed in assembling graphite dice under argon atmosphere, and then they were sintered at various conditions, e.g. sintering temperatures of 450–690 °C and duration of 5–30 min, in a hot-pressing vacuum furnace. The pressure in the die was kept at 25 MPa and the vacuum was 80 Pa in the furnace. After hot-pressing, the end-products were cut and polished. The structure of in situ phases formed in HPed specimens was investigated by X-ray diffraction(XRD) analyses. The microstructures of fracture surfaces of the composites were observed by scanning electron microscopy (SEM; JSM-5310) with an analytical energy dispersive X-ray spectrometer (EDX) system for local chemical composition analyses. XRD analyses were performed on a Rigaku D/max-II B X-ray diffractometer with CuKα (λ = 1.5406 Å) radiation, operating at 40 kV and 20 mA. The scanning speed was 0.02 °s^{-1}. The Archimedes technique was used to measure the density of each composite sample. Microhardnesses of the MMCs were measured by the microhardness tester FM-700(FUTURE TECH) with a load of 100 g and dwell time of 15 s. Tensile tests were performed on an Instron model 1125 test machine under 2 mm per min monotonic loading; the uniform gauge length of tensile test was 10 mm. Tensile specimens were cut from the hot-pressed composites.

Received: January 16, 2006
Final version: March 19, 2006

[1] M. Taya, R. J. Arsenault. *Met. Matrix Compos.* Pergamon Press, Oxford, **1989**.
[2] Peng Yu, Zhi Mei, S. C. Tjong, *Mater. Chem. Phys.* **2005**, *93*, 109.
[3] D. C. Jia, Y. Zhou, T. C. Lei, *Mater. Sci. Eng. A* **1997**, *232*, 183.
[4] L. Lu, M. O. Lai, C. W. Ng. *Mater. Sci. Eng. A* **1998**, *252*, 203.
[5] K. L. Tee, L. Lu, M. O. Lai, *Comp Struc.* **1999**, *47*, 589.
[6] C. Suryanarayana. *Progr. Mater. Sci.* **2000**, *46*, 1.
[7] J. S. Benjamin. *Metall. Trans.* **1970**, *1*, 2943.
[8] J. S. Benjamin. *Sci. Am.* **1976**, *234*, 40.
[9] P. S. Gilman, J. S. Benjamin. *Ann. Rev. Mater. Sci.* **1989**. *13*, 279.
[10] H. G Tang, X. F. Ma, W. Zhao, X. W. Yan, R. J. Hong, *J. Alloy Comp.* **2002**, *347*, 228.
[11] *ASM Met. Handbook*, eighth edition Vol.8. Metallography, structures and phase diagrams, **1973**.

DOI: 10.1002/adem.200600007

The Influence of Magnetic Fields on the Mechanical Behaviour of Granular Materials Used for Foundry Moulding: Numerical and Experimental Analysis**

By *Pierre-Marie Geffroy, Javier Goni, Xabier Pena, Dominique Bernard, Jean-François Silvain**

The aim of this study is to compare the mechanical behaviour of the mould with two innovative foundry processes; magnetic moulding using a cohesive granular material and the lost foam process. Understanding the mechanical behaviour of the mould will allow us to improve dimensional tolerances for complex shape castings and decrease defects due to mould collapse. Finite Element analysis allows us to calculate the magnetic field and distribution of magnetic cohesion in steel shot moulds – necessary to determine the optimum magnetizing equipment parameters. The advantages and mechanical characteristics of the magnetic moulding process are presented in this study and the main factors involved in this process are discussed.

With the magnetic moulding process,[2] the mould material must flow easily during the moulding stage and be rigid during the casting and the solidification stages. This suggests the use of an alternative mould material to unbonded sands typical of the lost foam process, meaning that the magnetic moulding process can be regarded as an extension of lost foam process. The steel shot is free flowing during the moulding stage and can be compacted by vibration. After compac-

[*] *Dr. P.-M. Geffroy, Dr. J. Goni, X. Pena*
Fundación INASMET
Mikeletegi Pasealekua
2, Parque Tecnológico, 20009 San Sebastián, Spain.
Dr. D. Bernard, Dr. J.-F. Silvain
ICMCB-CNRS, Université de Bordeaux1
87 Avenue du Docteur Albert Schweitzer, 33608 Pessac, France
E-mail: silvain@icmcb-bordeaux.cnrs.fr

[**] *This study was developed within the framework of a European Commission funded Project, Marie Curie fellowship contract number G1TR-CT-2000-00015. Moreover, the authors wish to express their gratitude to Knauf Creafoam (France) for the technical advice given on various aspects of foam patterns.*

